A study of ion injections at the dawn and dusk polar edges of the auroral oval

H. Stenuit,[1] J.-A. Sauvaud,[1] D. C. Delcourt,[2] T. Mukai,[3] S. Kokubun,[4] M. Fujimoto,[5] N. Y. Buzulukova,[6] R. A. Kovrazhkin,[6] R. P. Lin,[7] and R. P. Lepping[8]

Abstract. In the auroral dawn and dusk magnetosphere at altitudes of ~2-3 R_E, three distinct zones of ion and electron precipitation are commonly detected onboard Interball 2, near the polar edge of the auroral oval. From high to low latitudes the satellite encounters (1) magnetosheath/low-latitude boundary layer (LLBL) like plasma (Zone 1), (2) a mixing region with plasma characteristics between LLBL and plasma sheet (Zone 2), and (3) the auroral plasma sheet precipitation (Zone 3). Further equatorward, the satellite crosses the inner plasma sheet characterized by "ion gaps" in the morning sector. Inside Zones 1 and 2 impulsive ion injections are often detected. They consist of overlapping energy dispersed structures from about 10 keV down to several hundreds of eV with temperature close to that of the magnetosheath. Using trajectory computations backward in time, these dispersions are shown to be cause by time-of-flight effect from a distant source located close to the equatorial magnetopause. Whereas Zone 1 is located mainly poleward of region 1 (downward field-aligned currents at dawn and upward field-aligned currents at dusk), Zone 2 generally coincides with region 1. It is mainly located on closed field lines, as evidenced from the local detection of bouncing ion clusters. Finally, Zone 3 corresponds with region 2 of upward field-aligned currents. A statistical study of Zone 1 which is present in about 12% of the satellite passes at dawn and dusk reveals that its probability of occurrence seems to be controlled by the interplanetary magnetic field (IMF). That is, it is formed when the IMF has a northward component and tends to be radially directed. Moreover, it is more frequently encountered during periods of enhanced solar wind pressure. Detailed case studies uncover a remarkable correlation between the onsets of individual injections inside Zone 1 and those of pressure pulses in the magnetosheath. Both have a characteristic period of ~ 200- 250 s, similar to that of Pc5 events associated with these injections and detected on board Interball 2. Altogether, these observations indicate that injections and related Alfvèn waves are driven by magnetosheath pressure pulses associated with a quasi-parallel bow shock. The plasma penetration mechanism remains to be understood.

1. Introduction

Polar regions constitute the ionospheric projection of the magnetosphere plasma reservoirs and boundaries. In the dayside, near noon, data from low-altitude polar orbiting satellites first allowed to characterize the polar cusp [*Frank*, 1971] and the dayside extension of the plasma sheet [*Galperin et al.*, 1976]. Based on plasma characteristics, *Newell et al.* [1991] and *Newell and Meng* [1992] defined three regions in the vicinity of the cusp with magnetosheath-like particles: the cusp proper which is about 2.5 hours in total local time extent,

[1]Centre d'Etude Spatiale des Rayonnements, CNRS, Toulouse, France.

[2]Centre d'étude des Environnements Terrestres et Planétaires, CNRS, Saint-Maur des Fossés, France.

[3]Institute of Space and Astronautical Science, Sagamihara, Japan.

[4]STE Laboratory, Nagoya University, Nagoya, Japan.

[5]Department of Earth and Planetary Sciences, Tokyo Institute of Technology, Tokyo, Japan.

[6]Space Research Institute, Moscow, Russia.

[7]Space Science Laboratory, University of California, Berkeley, California, USA.

[8]NASA Goddard Space Flight Center, Greenbelt, Maryland, USA.

the low-latitude boundary layer (LLBL) which extends to about 09:00 magnetic local time (MLT), and the mantle which reaches to about 08:00/16:00 MLT. Outside the cusp, *Woch et al.* [1994] identified three regions: the projection of the magnetospheric low-latitude boundary layer (LLBL) with magnetosheath-like ion distribution, the plasma sheet (PS), and an overlapping region of LLBL and PS populations (called LLBL/SR).

More specifically, data from hot plasma instruments on board rockets and spacecrafts have shown that plasma with magnetosheath origin can be observed at auroral latitudes away from the noon sector, well into the dawn and dusk auroral magnetosphere [*Carlson and Torbert*, 1980; *Woch and Lundin*, 1991, 1992; *Clemmons et al.*, 1995; *Sandahl et al.*, 1998; *Sauvaud et al.*, 1998; *Ober et al.*, 2000]. The injected magnetosheath ions often exhibit characteristic energy/pitch angle dispersion previously reported for solar wind ions accessing the magnetosphere in the cusp regions. However, the dawn/dusk events appear as intermittent injections rather than as a continuous inflow of solar wind plasma. Using Viking observations, *Woch and Lundin* [1992] performed a statistical study of such plasma injections in the dayside auroral oval from about 06:00 MLT to 19:00 MLT and between 70° and 80° of invariant latitude, outside the polar cusp. They showed that their occurrence frequency is highest for radially directed interplanetary magnetic field (IMF). These authors also found a
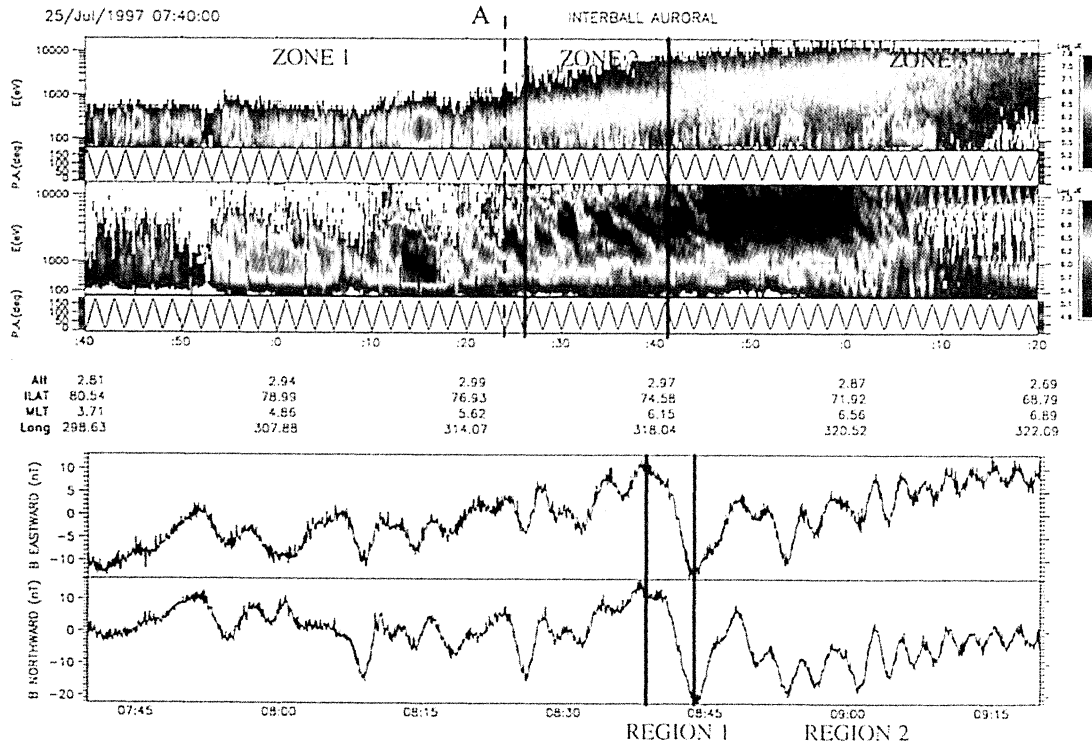
Plate 1. (top) Interball-Auroral data, electrons, protons energy-time spectrograms with the corresponding pitch angles between 0740 and 0920 UT on July 25, 1997. The energy fluxes are color coded. (bottom) The perturbation magnetic field east-west and north-south components in a magnetic field-aligned reference frame.
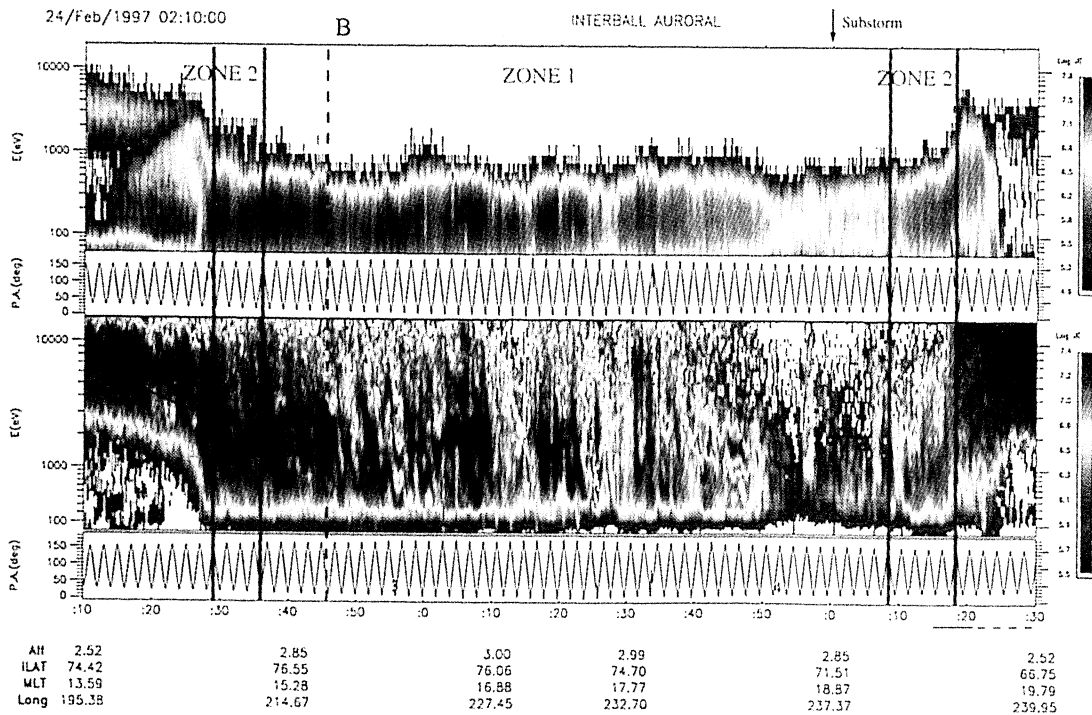

Plate 2. Injection case in the duskside of the auroral magnetosphere. Electron and protons energy-time spectrograms and the corresponding pitch angles on February 24, 1997, between 0210 and 0430 UT. The fluxes are color coded. A substorm occurred at 0400 UT after a very quiet period. The solid line between 0210 and 0227 UT indicates the ion energy variation expected from a Fermi-type acceleration.

correlation between plasma injections and increased solar wind pressure. They concluded that transient reconnection events could not be regarded as the main source of the dawn/dusk magnetosheath-like precipitation.

The Interball and International Solar Terrestrial Physics (ISTP) databases allow us to perform more detailed studies of these ion injection events using, when possible, simultaneous data taken in the solar wind (Wind or Interball-Tail), in the magnetosheath, downstream of the bow shock (Geotail) and over the polar regions of the magnetosphere (Interball-Auroral). The data obtained from the ION experiment on board the Interball satellite lead us to identify three distinct precipitation regions in the morning and evening sides of the auroral oval, as already reported by *Woch et al.* [1994]: the LLBL/magnetosheath-like Zone (Zone 1), the PS (Zone 3), and a transition region between LLBL and PS (Zone 2) characterized by an increase of the electron energy from LLBL-like to plasma sheet-like (Plate 1). Interball-Aurora data show that in the first two regions well-structured ion precipitation due to time of flight effects are generally detected, while such energy dispersion are less frequent in Zone 3. The three zones are shown to have very different occurrence probabilities, the smallest one (12%) corresponding to Zone 1 which we show to be in most cases located poleward of the downward field-aligned currents of Region 1.

For this study we focus on ion injections in this first zone. Here a strong asymmetry is found between dawn and dusk sectors, the injections being about 3 times more frequent at dawn. In both sectors they occur preferentially for positive IMF B_z component. This study also shows that injections are seen for opposite IMF B_y component at dawn and at dusk. We examine how this result could fit the recent works of *Nishikawa* [1998] and *White et al.* [1998]. For several cases, when Interball and Geotail showed good conjunctions, a striking correlation is found between repetitive pressure pulses detected inside the magnetosheath and sporadic plasma entry events detected over the auroral region at 2-3 R_E altitude. Associated with these pressure variations, Pc5 pulsations are systematically recorded. Altogether these observations suggest a penetration process that is closely linked to both IMF direction which controls the nature of the Earth bow shock and magnetosheath pressure pulses (these being ultimately linked with the bow shock properties).

2. Data Sources

This study is primarily based on ION and magnetic field (IMAP-3) experiments flown on board the Interball-Auroral spacecraft, launched in August 1996 into a 62.8° inclination orbit with an apogee of ~ 3 R_E. The satellite orbital period is ~6 hours. It is spinning at a rate of 0.5 rpm. Near apogee, the spacecraft slowly (~ 1 km s^{-1}) skims through the dawn and dusk sectors at altitudes of the order of 2-3 R_E, hence providing a unique opportunity to study signatures of magnetosheath plasma penetration through the magnetopause.

The ION experiment was developed to measure both auroral ions and electrons. This experiment consists of two mass spectrometers (Wien filters) and two simple electron detectors [*Sauvaud et al.*, 1998]. The mass spectrometers are looking in opposite directions, perpendicularly to the satellite spin axis that points toward the Sun. They measure H$^+$ and O$^+$ ions in the energy range ~0 - 14,000 eV Q^{-1}. The two electron spectrometers are also looking in opposite directions and perform measurements in the energy range ~10 - 20,000 eV.
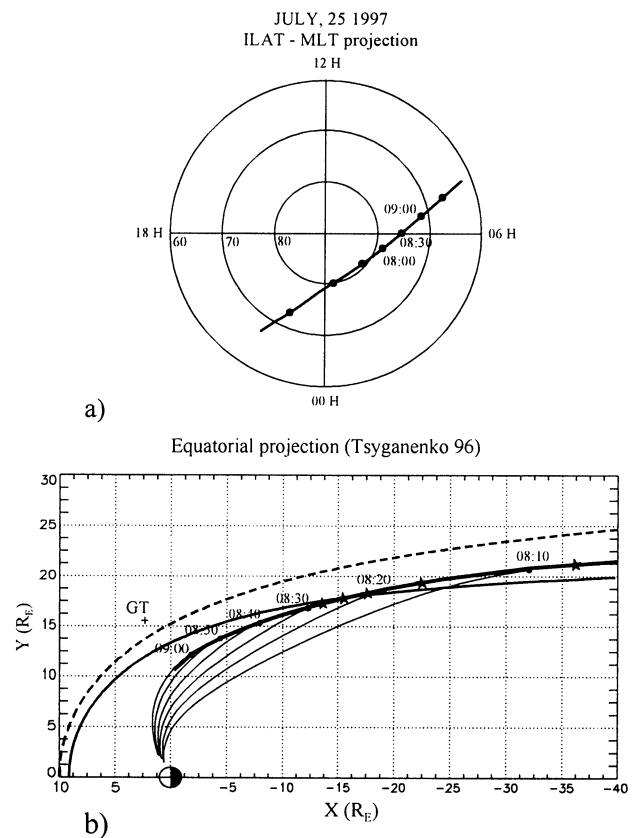

a)

b)

Figure 1. (a) IA orbit in a magnetic local time-invariant latitude frame. (b) IA orbit projected into the magnetospheric equatorial plane using the Tsyganenko 1996 magnetic field model. Magnetic field lines of the Northern Hemisphere, which are connected between the region observed by IA and the equatorial plane, are also shown by a solid line. The shift toward dayside of the magnetic field lines ending points near the Earth (comparing with Figure 1a) is due to the Earth axis inclination and to the satellite altitude (~3 R_E). The magnetopause shape is computed from the *Shue et al.* [1998] model for two different dynamic pressures pertaining to the considered period.

The time required to sample a full energy spectrum vary from 1.5 to 6 s depending on the operation mode. The magnetic field vector is given by IMAP-3, a fluxgate sensor with a time resolution which can be varied between 1/16 and 3 s, this latter resolution being used throughout this paper [*Arshinkov et al.*, 1995]. Interball data were correlated with plasma and magnetic field measurements from the Low-Energy Particle Electrostatic Analyzer (LEP-EA) and magnetic field (MGF) instruments installed on board Geotail. Detailed descriptions of these instruments are given by *Mukai et al.* [1994] and *Kokubun et al.* [1994], respectively. In the present analysis we use data averaged over four spin periods (about 12 s) for LEP-EA and spin averaged data for MGF. Wind plasma and magnetic field data used throughout the paper come from the 3-D Plasma and Energetic Particle Analyser (3DP) and Magnetic Fields Investigations (MFI) instruments, respectively, as described by *Lin et al.* [1995] and *Lepping et al.* [1995]. Wind data have generally been averaged over 1 min for statistical analysis. Some correlations were made with the magnetic field measurements on board Interball-Tail with the Multi-component Investigations of Fluctuations of Magnetic Fields (MIF-M) magnetometer experiment [*Klimov et al.*, 1995].
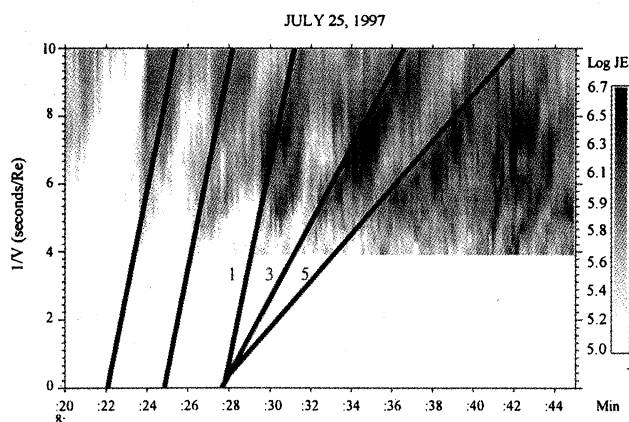
JULY 25, 1997

Figure 2. Inverse-velocity/time spectrogram for July 25, 1997, between 0826 and 0845 UT. After initial injections (~0828 UT) the following dispersed structures correspond to bouncing ion clusters.

3. Observations

3.1. Dawnside: July 25, 1997

Plate 1 displays electron and hydrogen energy-time spectrograms and their corresponding pitch angles for a typical polar pass on July 25, 1997, between 0740 and 0920 UT when a series of ion injections are detected by Interball-Auroral (therein referred to as IA) in the dawnside of the auroral oval. Energy fluxes are color coded. The bottom panels give the eastward and northward magnetic field residuals measured on board IA. The field-aligned component, which exhibits smooth variations, is not shown. Figure 1a shows the orbit of IA in a magnetic local time – invariant latitude frame, while Figure 1b illustrates the projection of the IA orbit into the magnetospheric equatorial plane along the Tsyganenko 1996 magnetic model field lines [*Tsyganenko*, 1995; *Tsyganenko and Stern*, 1996]. In Figure 1b the dashed line represents the average magnetopause location for the observation period calculated from the Shue model [*Shue et al.*, 1997, 1998]. The solid line indicates the extreme magnetopause position for higher dynamic pressures pertaining to the studied period (see section 5.1). Before 0740 UT, IA was first in the polar cap, flying sunward and equatorward when it crosses a first zone between ~ 0740 and ~ 0827 UT, at latitudes between 80° and 76° (Figure 1a). This zone is characterized by bidirectional low-energy electrons ($E <$ 1 keV) appearing sporadically over a more diffuse precipitation (see Plate 1). However, the slow spin of the satellite does not enable us to unambiguously disentangle the electron flux time variations from pitch angle variations. The ion fluxes are more structured with a tendency for the energy to decrease with time. Inside this zone, data from the energetic particle experiment DOK-2 on board IA [*Lutsenko et al.*, 1995] indicate that energetic ion and electron flux between 20 and 800 keV is near background. Moreover, for this case, inside Zone 1 ionospheric oxygen ions are flowing upward with energies which can reach 1 keV (not shown). A statistical study shows that this oxygen up flow is a common feature of Zone 1. The satellite then crosses a second zone between 0827 and 0842 UT with a mixture of low-energy electrons and plasma sheet electrons (Plate 1). The electron temperature is steadily increasing inside this latter region. Similar measurements of mixed LLBL and plasma sheet electrons have been reported as a characteristic feature of the flank magnetosphere, near the equatorial plane

[e.g., *Sauvaud et al.*, 1998]. This suggests that the spacecraft passes through a region that can be viewed as the auroral projection of low-latitude boundary layer (LLBL). Note that here the ion energy fluxes display clear successive energy-time dispersions. Then at 0842 UT, IA reaches the auroral plasma sheet characterized by an electron temperature in the keV range, the ion precipitation being here more diffuse. From 0908 UT, IA detected a nearly monoenergetic (around 4 keV) ion flux dropout. Such ion gaps are frequently observed in the dayside magnetosphere. They have already been interpreted as the result of magnetospheric residence times of ions exceeding their lifetime, which is controlled by charge exchange and wave particle interactions. This interpretation is supported by numerical orbit calculations which show that ions originating from the magnetotail exhibit extremely large times of flight in a limited energy range due to the conflicting effects of $E \times B$ and gradient drifts [*Sauvaud et al.*, 1998; *Kovrazhkin et al.*, 1999]. This region corresponds to quasi-dipolar field lines.

Starting around 0753 UT, inside the first and second zones, IA observed hydrogen energy/pitch angle structures. Inside each structure the energy decreases from 10 keV down to several hundred eV and shows a weak pitch angle modulation. Both signatures are due to time of flight effects. However, the most poleward structure seen between 0740 and 0750 does not exhibit a clear energy dispersion. During this 10 min interval, the IA orbit projection was located beyond $X = $ -40 R_E into the equatorial plane (Figure 1b) and the satellite was traveling very fast along the magnetopause. Accordingly, the observed structure can not be assigned to a well-defined region on the magnetospheric flanks and space and time variations are highly related. Starting around 0752 UT, that is, when the IA projection slower moves along the magnetopause, the following events present repeated injections that possibly overlap. In the second region, injections become more energetic. Between 0820 and 0832 UT, injections appear about every 3 or 4 min while their duration is around 5 min. For given energy the width of the structure is about 2 min, which must be related to the injection duration in the outer magnetosphere. A fundamental difference was found between ion structures detected before and after 0828 UT. When displayed in a inverse velocity-time diagram, ion traces occurring before 0828 UT are best fitted by parallel lines, while later, ion traces converge toward the same injection time (Figure 2). IA thus observes bouncing ion clusters in Zone 2, which is a strong indication that the corresponding field lines are closed. In contrast, the first two injections in Zone 2 cannot be identified as bouncing ion clusters. At this point it must be realized that these ions registered at the poleward edge of Zone 2 (defined from fast electron characteristics) are slowly moving along field lines so that they have been injected from the magnetosheath/LLBL several minutes before their observation, that is, while the satellite was in Zone 1.

The bottom panel of Plate 1 gives the variations of the magnetic field residuals. Between 0839 and 0842 UT the eastward component presents a sharp decrease which indicates the crossing of Region 1 of downward field-aligned currents. Afterwards, the slow increase of the azimuthal component marks the encounter of Region 2. A remarkable feature here is the presence of waves with periods corresponding to Pc5 pulsations ($T \sim 250$ s). The polarization of these waves is linear and oriented mainly east-west with a small north-south component. These waves are intensified between 0820 and 0829 UT, that is, in Zones 1 and 2. They can be detected also in Zone 3 with smaller amplitude. More generally, it is only
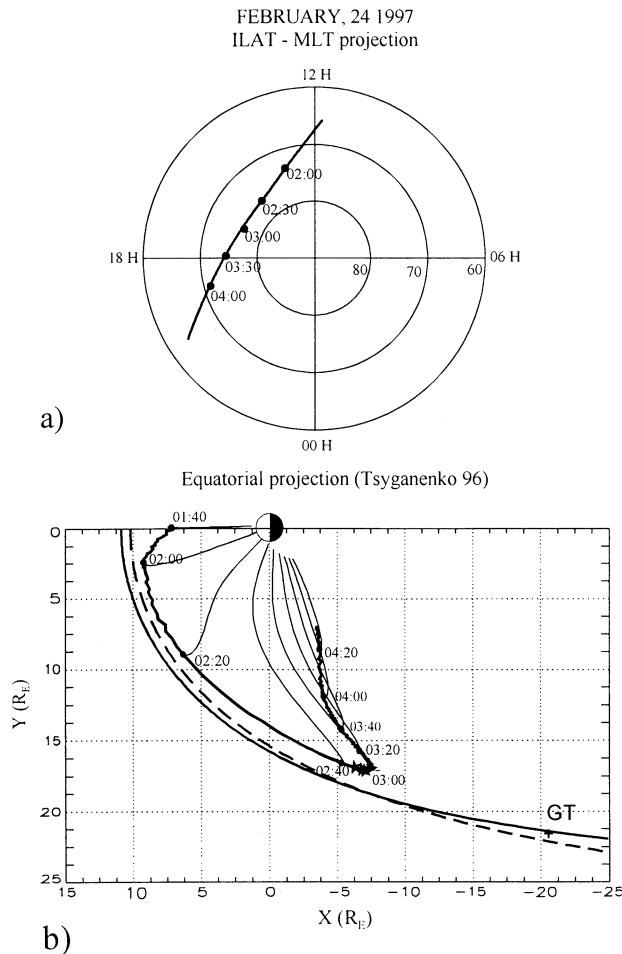
FEBRUARY, 24 1997
ILAT - MLT projection

a)

Equatorial projection (Tsyganenko 96)

b)

Figure 3. (a) IA orbit on February 24, 1997, in a magnetic local time-invariant latitude frame. (b) IA orbit projected into the magnetospheric equatorial plane using the Tsyganenko 1996 magnetic field model. Magnetic field lines of the Northern Hemisphere, which are connected between the region observed by IA and the equatorial plane, are also shown in solid line. The shift toward nightside of the magnetic field lines ending points near the Earth (comparing with Figure 3a) is due to the Earth axis inclination and to the satellite altitude ($\sim$3 R_E). The magnetopause shape is computed from the *Shue et al.* [1998] model for two different dynamic pressures pertaining to the considered period.

when such low-frequency waves present a large amplitude in Zone 3 that the associated ion fluxes show typical time-of-flight dispersed structures.

A survey of the IA data reveals that the boundary between field-aligned currents of Region 1 and Region 2 lies inside Zone 2 (transition region between magnetosheath/LLBL and plasma sheet). Region 1 is not always exactly restricted to Zone 2 as for the case presented here and can extend into Zone 1. In contrast, when Zone 1 is absent, Region 1 exactly coincides with Zone 2. This result is in agreement with the recent work of *Farrugia et al.* [2000], who suggest that the source for Region 1 may be the region they called the mixing region corresponding to our Zone 2. However, they contrast with the results of *Newell et al.* [1991] who found in a small number of instances that R1 corresponds to LLBL. As stressed by *de la Beaujardiere et al.* [1993] who proposed that R1 straddled the open/closed boundary, the relation between the field-aligned currents and

the particles boundaries is variable and depend on the criteria for particle identification, which are by necessity different for each study.

3.2. Duskside: February 24, 1997

A case of ion injections at dusk is shown in Plate 2, which displays electron and proton energy-time spectrograms and their corresponding pitch-angles between 0210 and 0430 UT on February 24, 1997. As for the preceding example, Figure 3a gives the orbit of IA in a magnetic local time – invariant latitude frame, while Figure 3b illustrates the IA projection into the magnetospheric equatorial plane along the Tsyganenko 1996 model magnetic field lines. Coming from the noon sector, IA first encounters plasma sheet proton population before 0229 UT, then briefly reaches Zone 2 between 0229 and 0235 UT and stays in Zone 1 from $\sim$0235 to $\sim$0337 UT. From 0337, ion injections cease. At the same time, large-amplitude compressional waves with a period of $\sim$3 min are detected (not shown). These can result from global compression of the magnetosphere that takes the satellite out of Zone 1. Finally, IA enters again Zone 2 at 0408 UT and encounters the auroral plasma sheet in the evening side of the oval at $\sim$0418 UT. According to the provisional *AE* index from World Data Center 2 (WDC-2) and to the ground magnetic field measurements at Narssarssuaq a substorm onset occurs around 0400 UT.

During the first auroral plasma sheet encounter in the dayside, before 0229 UT, the ion energy shows a characteristic behavior, that is, it slowly decreases as the invariant latitude increases. This energy change can be simply understood as plasma heating inside the plasma sheet [see *Galperin et al.*, 1978; *Sauvaud et al.*, 1981]. Inside the magnetosphere the ion average energy is expected to vary as $1/L^2$, where L is the field line length, due to conservation of the second adiabatic invariant:

$$J = 2\oint m V_{//} dl \approx < V_{//} > L \Rightarrow E \propto 1/L^2 .$$

On the left side of Plate 2, the black solid line represents the predicted $1/L^2$ dependence expected from the *Tsyganenko* [1989] magnetic field model for a magnetic index Kp= 2. The agreement between the data and the model is satisfactory.

Zone 1 contains numerous and mixed ion energy/pitch angle structures, a close inspection of these structures show that they are produced by time-of-flight dispersion effects. This point will be examined in more details hereinafter (section 5.2). The corresponding electron population is restricted to energies lower than about 1 keV. Their energy spectra are quite similar to those of LLBL electrons.

For this case, telemetry problems affect magnetic field measurements, so that it is possible to locate Regions 1 and 2 only in the evening portion of the pass. Their position is given in Plate 2 by horizontal full and dotted horizontal lines.

3.3. Proton Spectra Comparison

The energy spectra of the source of protons in Zones 1 and 2 can be found from the envelope of superposed individual spectrum within individual dispersed structures. Note, however, that only ions with small initial pitch angles (< 4° for a source field of 40 nT) are able to reach the IA altitude. Figure 4 presents the spectrum of this "field-aligned" source. For comparison a typical cusp spectrum obtained on board is also shown. The temperature of the ions inside the energy-dispersed
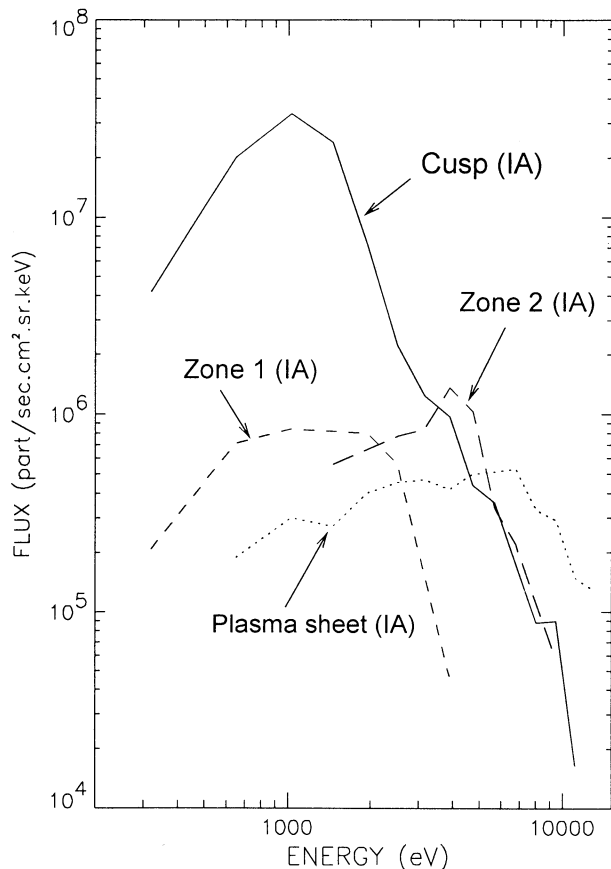
Figure 4. Comparison of ion energy spectra in the cusp (Interball-Auroral) and in the three zones detected by IA on July 25, 1997 (see text).

order not to confuse the magnetosheath-like injections with substorm related time of flight dispersion of plasma sheet ions [*Sauvaud et al.,* 1999]. The event selection was also performed on the base of the ion and electron energy spectra. Events exhibiting nightside plasma sheet-like particle distributions were excluded. The satellite passes in the near-noon region were excluded too in order to discard the "direct" solar wind particle entry inside the dayside cusp. We finally selected 131 cases of injections of the Zone 1 type. This represents about $\frac{2}{5}$ of all injection events (Zones 1, 2, and 3) and 12% of the passes. Most cases were found between 5 and 8 hours MLT and between 14 and 17 hours MLT. Seventy nine percent (104 cases) of the events occur in the dawnside of the auroral oval and 21% (27 cases) in the duskside. This $\frac{4}{5}$, $\frac{1}{5}$ proportion is not an artifact of our statistics since the satellite has performed measurements for nearly the same number of orbits at dawn and at dusk, 562 and 533, respectively. Most of the events are detected during quiet times.

4.1. Relation With the Interplanetary Magnetic Field Configuration

In this first part of the statistical study we wish to check if injection events in Zone 1 are controlled by the IMF orientation. IMF data principally come from the Wind spacecraft. However, when possible, Geotail data were also used. After introducing appropriate time delays for the solar wind to reach the magnetosphere ($X_{GSM} = 0$), the IMF GSM component values were averaged over the injection observation period, which generally does not exceed 1 hour. For comparison a statistical study of the IMF component given by Wind was also performed to determine the general IMF orientation. This was done by averaging the IMF data over 1 hour intervals for a total of 6 months randomly taken during the 2 years corresponding to the IA data. As a result, the IMF B_z is in average slightly more negative (57%) than positive (40%).

Figure 5 displays the same information for periods corresponding to ion injections into Zone 1 with a subdivision corresponding to injections at dawn and at dusk. The occurrence frequencies were obtained by dividing the number of injections at dawn and at dusk by the total number of injections in these respective sectors. The top panel of Figure 5 when compared to the statistical study of the IMF component indicates without ambiguity that Zone 1 is mainly detected in both the dawn and dusk sectors for positive IMF B_z. This result could be related to the finding by *Mitchell et al.* [1987] that the LLBL is thicker for northward IMF.

The bottom panels of Figure 5 represent the normalized relative occurrence frequency of the angle between IMF B_z and GSM XY plane. The normalized relative occurrence frequencies where calculated by normalizing the number of injections for each angle interval to the number of cases in the average statistic for the same angle interval. The bottom panels of Figure 5 clearly indicate that injections preferentially correspond to northward IMF and to a large positive inclination of the IMF over the ecliptic plane.

The dependence of the injection occurrence with the direction of the interplanetary magnetic field in the ecliptic plane is given in Figure 6. The top panel displays the average magnetic field occurrence probability for different angular sectors as deduced from Wind data. As expected, the IMF direction is centered to the direction of the solar Archimede spiral, given here for the average solar wind velocity pertaining to the measurements: 380 km s^{-1}. The two other panels display
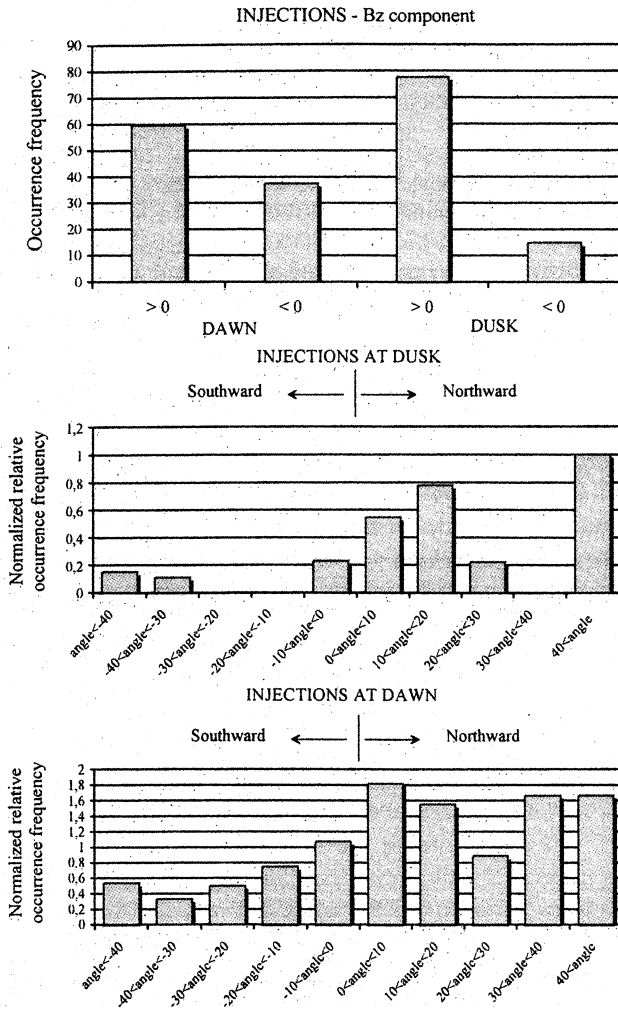
structures of Zone 1 (spectrum from July 25, 1997, 0824-0828 UT) is quite similar to that of typical cusp ion energy spectrum. Fluxes are reduced by a factor of the order of 40. This leads us to conclude that the ultimate source of these ions is the magnetosheath. Note also that Zone 2 (spectrum from July 25, 1997, 0832-0837 UT) presents a spectrum intermediate between the spectra of the first and the third zone. The energy spectrum of Zone 3 (spectrum from July 25, 1997, 0856-0858 UT) is similar to that of the plasma sheet.

4. Statistical Study

From the IA database it appears that Zone 1 never appears at latitudes below 75°. For latitudes higher than 75°, Zone 1 is only occasionally detected. As a result, the satellite can come from the polar cap, and directly enter into Zone 2 before going into the low-altitude plasma sheet. Furthermore for some orbits we observe the presence of low-energy electrons of Zone 1 type but with no detectable ion fluxes. On the contrary, Zone 2 is detected with more or less structured ion injections in almost all orbits. For this statistical study we focus on the ion injections in Zone 1, which is linked either to the more exterior part of the magnetosphere or to the magnetosheath. Such events were identified from October 1996 to June 1998. This selection corresponds to the dawnside and duskside of the auroral oval for magnetic local times between 3 and 11 hours at dawn and between 13 and 21 hours at dusk. The invariant latitude range is 75° - 80°. The midnight sector of the oval was excluded in

INJECTIONS - Bz component

INJECTIONS AT DUSK

Southward ←——— | ———→ Northward

INJECTIONS AT DAWN

Southward ←——— | ———→ Northward

Figure 5. (top) Sign of the IMF B_z component corresponding to the injection events inside Zone 1. Angle between the IMF B_z component and the *XY* GSM plane during Zone 1 encounters (middle) at dusk and (bottom) at dawn.

the same information for the injections at dusk and at dawn. The IMF orientation corresponding to Zone 1 occurrence tends to be more radial than usual. At dawn the injections occur more often for a duskward and tailward IMF component: 44% for duskward and tailward against 27% for dawnward and sunward. The opposite configuration is found for dusk injection events. In view of the recent works of *White et al.* [1998] and *Nishikawa* [1998] about the particle entry through reconnection grooves in the magnetopause for pure B_y IMF, our statistics would imply that ions have entered the magnetosphere in the Southern Hemisphere and follow the magnetic field lines connected up to Interball located at the Northern Hemisphere. Still, the tendency for the IMF to be more radially directed during injections than usually could indicate that the Earth bow shock in the vicinity of the subsolar point is quasi-parallel, suggesting a more turbulent magnetosheath than in the case of perpendicular shock [*Sibeck et al.,* 1989a, 1989b].

These results imply a mode of interaction between the solar wind and the magnetosphere whereby plasma changes produced in the foreshock subsequently convect through the bow shock and impinge on the magnetosphere [*Fairfield et al.,* 1990]. Furthermore, it has been shown by *Russell et al.* [1983] that

waves generated at the bow shock and propagating mainly along magnetosheath streamlines have a higher probability of reaching the magnetopause for small values of the angle between the IMF and the shock normal near the subsolar point ($\theta_{BN} < 30°$). Still, due to the average orientation of the IMF, the upstream waves are more likely convected to the morning flank of the magnetosphere.

4.2. Relationship With the SW Dynamic Pressure

Statistics made on the average velocity and average dynamic pressure of the solar wind corresponding to injection events reveal that these parameters are close to the average velocity (~380 km s^{-1}) and the average dynamic pressure (~2 nP) of the solar wind. However, when normalized, injections in Zone 1 show a weak increase of occurrence for high dynamic pressures, in the range 2.5-4.5 nP (Figure 7). For dynamic pressures higher than 4.5 nP the number of cases is not significant. These results are in agreement with those of *Woch and Lundin* [1992]. These authors found that the event occurrence is independent of the solar wind velocity and that the probability of observing injection events increases when the solar wind dynamic pressure is higher than usual. Moreover, Woch and Lundin examined the dependence on dynamic pressure for cases with IMF closer to the azimuthal and closer to the radial direction. The dependence is more pronounced when the IMF is radially directed.

5. Relationship With Magnetosheath Dynamic Pressure Pulses

For several injection events, Geotail was located inside the magnetosheath in the same local time sector as IA and close to the projection of the latter into the equatorial plane. We were thus able to look for correlation between ion injections and magnetosheath plasma parameters.
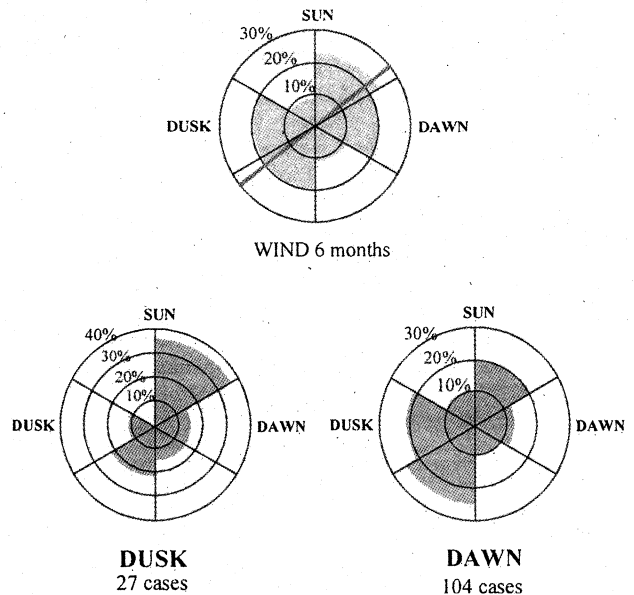

WIND 6 months

DUSK
27 cases

DAWN
104 cases

Figure 6. (top) Direction of the IMF in the *XY* GSM plane for a 6 months reference period. The wide gray line represents the average direction of the Archimede spiral computed for a solar wind velocity of 380 km s^{-1}. (bottom) Direction of the IMF in the *XY* GSM plane for ion injections in Zone 1, (left) at dusk and (right) at dawn.
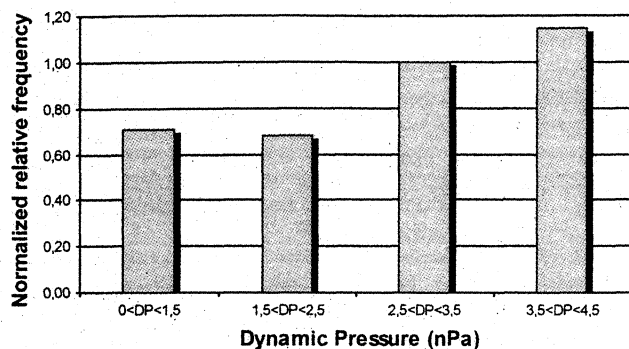
Figure 7. Solar wind dynamic pressure normalized distribution corresponding to ion injections into Zone 1.

5.1. July 25, 1997

The general characteristics of this injection event are displayed in Figure 8. This Figure presents the IA ion spectrogram, the dynamic pressure and the B_z component of the magnetic field measured in the magnetosheath by Geotail (X_{GSM}= 3, Y_{GSM}= -15, Z_{GSM}= 5) together with the IMF B_z component measured on board Wind in the solar wind close to the Earth (X_{GSM} = 15, Y_{GSM} = 16, Z_{GSM} = -7) and shifted in time. In order to verify that individual dispersed ion structures were mainly due to time-of-flight effects and to find their source with respect to the magnetospheric equatorial plane, they were traced backward in

time using a single particle trajectory code with the 3-D Tsyganenko 1996 magnetic field model [see *Delcourt et al.,* 1989]. As a main result, we found that ions from single injections inside Zone 1 and in the most poleward part of zone 2 come from a source located in the distant outer magnetosphere, near the equatorial plane. This result is illustrated in Figure 9, which presents the backward tracing for the injection beginning at 0824 UT and noted A in Plate 1. The two top panels of Figure 9 display the measured proton spectrogram and the corresponding pitch angle for an individual dispersed structure. The trajectories of particles forming the core (maximum energy flux) of the dispersion have been computed backward in time and represented with different black lines. The computed distance from the Earth, the magnetic local time, the SM latitude, the evolution of the ion pitch angles are indicated. Note that the focal point represents the approximate location of the source of the injected particles. The existence of a focal point at low latitudes indicates that ions were ejected nearly simultaneously, close to the equatorial plane (for a SM latitude in the range $0° - 15°$). Furthermore, we checked that the source region is located very close to the magnetopause (Figure 1b). Computation tests including electric field convection models were also performed. They showed that the addition of an electric field does not change significantly the results. Assuming that the ion injections are the result of a penetration mechanism on the equatorial magnetosphere, backward computations give for each energy an estimation of the time difference T_1 between the IA observations and the
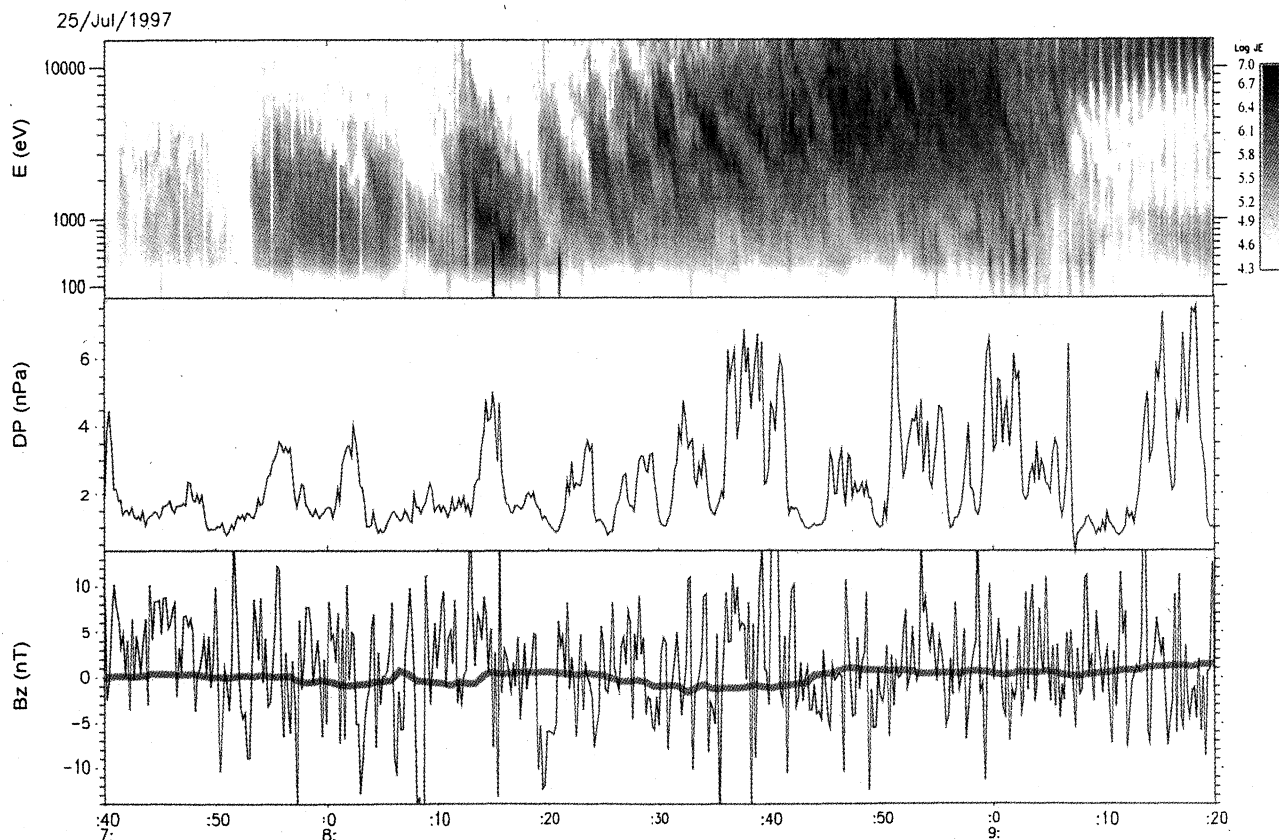

Figure 8. From top to bottom, the proton energy time spectrogram taken on board IA on July 25, 1997, the magnetosheath pressure variations measured on board Geotail, the magnetosheath (Geotail) B_z component of the magnetic field with superimposed solar wind (Wind) magnetic field measurements (see text).

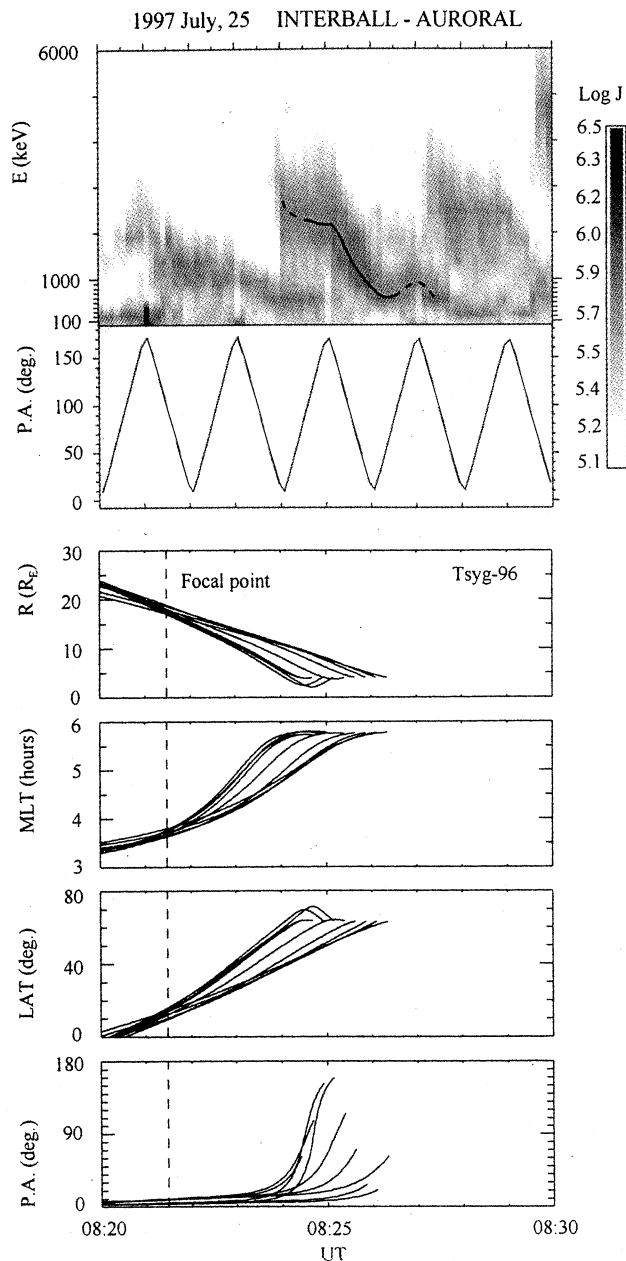1997 July, 25 INTERBALL - AURORAL

Figure 9. Details of the backward trajectory computations for the injection beginning at 0830 on the 25 July 1997 (noted A in Plate 1). The trajectories of particles (represented with different black lines) are computed backward in time from the shape of the energy/pitch angle time-of-flight dispersed structures. The solid line in the spectrogram represents the core of the dispersion (maximum energy flux). The *Tsyganenko* [1995] magnetic field model is used for 3-D computations. From top to bottom, energy-time spectrogram, corresponding ion pitch angle, distance from Earth (Earth radii), MLT (hours), magnetic latitude (degrees), and evolution of the pitch angle (degrees).

Knowing the intersatellite distance and the magnetosheath flow velocity, we computed the time delay T_2 for a plasma structure to travel between Geotail and the Interball equatorial projection. With T_1 and T_2 for several injections we can infer a relationship between the times of Geotail and IA observations. The top panel of Figure 10 gives the time delay necessary for 3 keV particles to reach IA starting from Geotail, as a function of UT on IA. Asterisks give the time delays derived from the method described above, and the black curve is the best fit to the "data" points. The bottom panel of Figure 10 illustrates the variations of the dynamic pressure measured on board Geotail in the magnetosheath (solid thick line) and the fluxes of the hydrogen ions at 3 keV (solid thin line) and 2 keV (dotted line) measured by IA. We used the computed time to display the IA data. Pressure and flux data were normalized to their respective norm. A cross-correlation analysis indicates that the correlation coefficient reaches 0.8. It appears that the best correlation is obtained for injections/pressure pulses occurring when the equatorial projection of IA is not too far from the Earth along the X axis (Figure 1b). The poorest agreement between the two curves is found for the injection beginning at 0811 UT. Here the width of the injection is about 10 min at 2 keV and includes the two pressure pulses at 0813 and 0817 UT. The good agreement between pressure variations in the magnetosheath and the ion flux variations measured on board IA strongly suggests that magnetosheath pressure pulses lead to sporadic
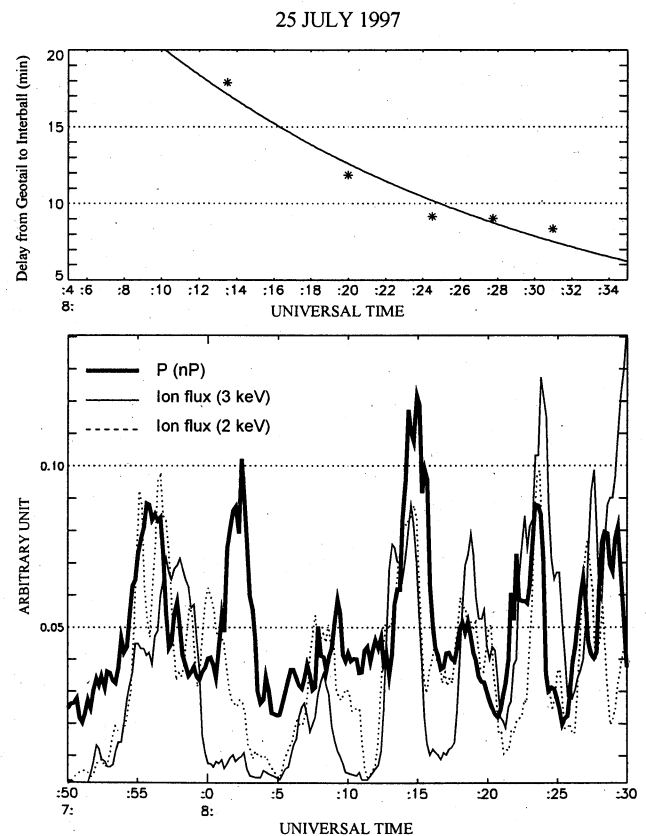

Figure 10. (top) Time delay for a 3 keV particle to travel from Geotail to IA as a function of UT on July 25, 1997. The points result from calculations (see text). The curve is a best fit. (bottom) Correlation between the dynamic pressure measured on board Geotail in the magnetosheath (solid thick line) and the proton ion fluxes at 3 keV (thin solid line) and 2 keV (dotted line). Time delays have been taken into account. The correlation coefficient reaches 0.8.
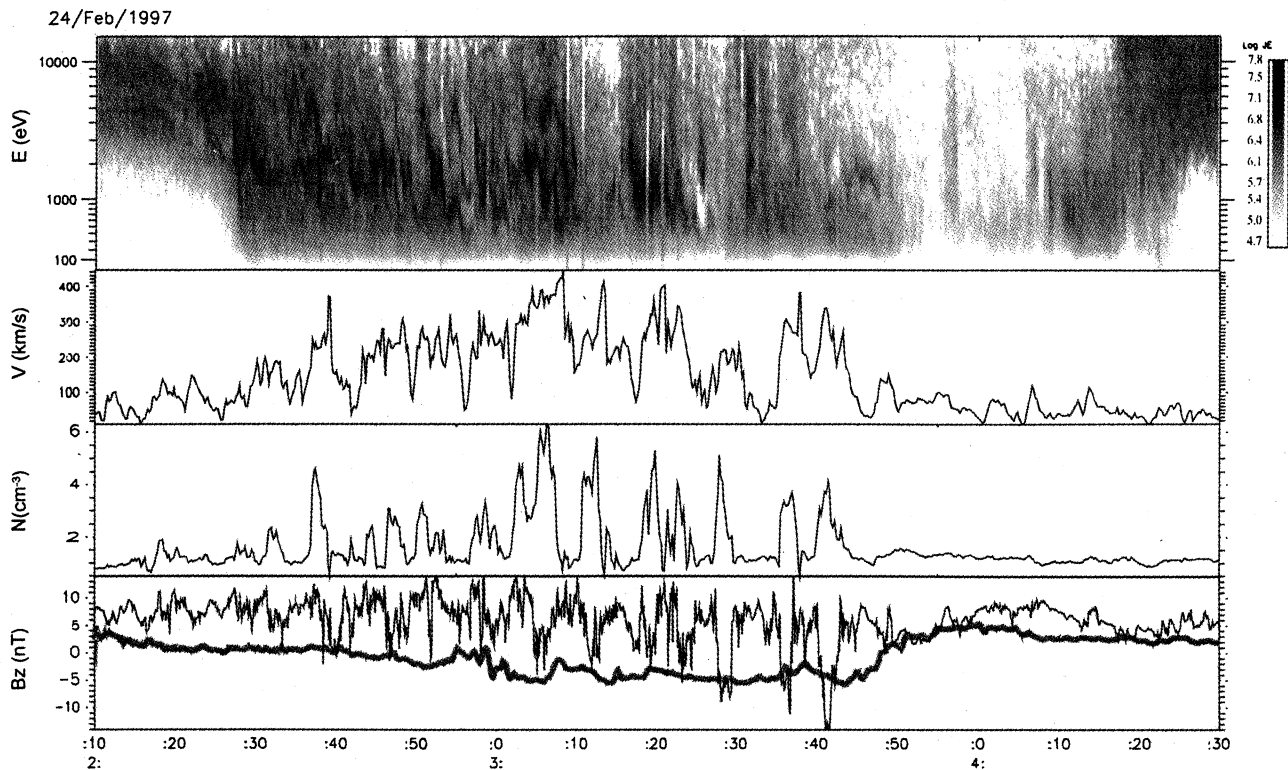
source location on the magnetopause, that is, the magnetospheric travel time. The stars in Figure 1b which display the equatorial projection along the magnetic field lines of the IA orbits using the Tsyganenko 1996 magnetic field model correspond to time T_1 for each injection time.

Note in Figure 1b that the projection of the IA orbit and Geotail (GT) are both located very close to the magnetopause.

Figure 11. From top to bottom, the proton energy time spectrogram taken on board IA on February 24, 1997, the magnetosheath plasma velocity and density variations measured on board Geotail, the magnetosheath (Geotail) B_z component of the magnetic field with superimposed solar wind (Interball-Tail) magnetic field measurements (see text).

injections of magnetosheath ions when the IMF has the appropriate orientation. It must be stressed that these variations of the plasma characteristics in the magnetosheath on the scale of minutes to tens of minutes are known to be several times larger than those of the solar wind plasma [e.g., *Zastenker et al.*, 1999]. As a matter of fact, for this day, no significant pressure pulses were seen in the solar wind by Wind.

It must be stressed that during the ion injections the magnetic field measured in the magnetosheath on board Geotail shows large-amplitude, low-frequency wave activity (Figure 8). The turbulence is highly compressive, and this very disturbed magnetic field does not show a preferential field direction.

5.2. February 24, 1997

The general characteristics of this injection event as detected on board IA are displayed in Plate 2. Figure 3b gives the respective positions of Geotail, of the equatorial projection of IA together with the model magnetopause of *Shue et al.* [1997, 1998]. Figure 11 provides further insights into the correlation between IA and Geotail observations. The IA proton energy spectrogram is displayed together with the magnetosheath plasma velocity, density, and B_z component of the magnetic field measured on board Geotail ($X_{GSM} = -21$, $Y_{GSM} = 20$, $Z_{GSM} = 7$) between 0210 and 0430 UT. The IMF B_z component measured by Interball-Tail ($X_{GSM} = 3$, $Y_{GSM} = 20$, $Z_{GSM} = 19$) is superimposed on Geotail magnetic measurements. Note that during this period, Geotail underwent a series of passes from LLBL to magnetosheath and backward, magnetosheath episodes being characterized by largest values of the plasma velocities and densities. The IMF B_z component was first positive until around 0255 UT. It subsequently turned slowly

negative and became positive again around 0345 UT. Ion injections are seen on board IA for both positive and negative B_z. Between 0240 and 0340 UT the IMF B_z quite closely corresponds to the B_z measured on board Geotail when it moved into the magnetosheath. The B_x and B_y components (not shown) display a turbulent behavior. It should be noted that the fast magnetopause motions are linked to increase dynamical pressure in the magnetosheath and that when Geotail is in the magnetosheath this corresponds to episodes of high pressure. However, we expect only major pressure pulses to be seen by Geotail, that is, those which are able to push the magnetopause earthward of the spacecraft.

In a like manner to the July 25, 1997, event, backward computations of IA energy dispersed structures were performed. Figure 12 gives an example of the results obtained for the injection occurring at 0247 (denoted B in Plate 2). Again taking into account several injections, we obtained a time correction to be applied to the IA data, in order to derive a correlation between the dynamic pressure measured by Geotail and the ion flux measured on board IA (Figure 13). As for the July 25, 1997, case, the correlation is satisfactory, although not perfect.

Between 0330 and 0350 Geotail goes in and out of the magnetosphere 6 times, around 0333, 0334, 0340, 0342, 0345, and 0348 UT. For these six crossings we were able to determine the normal vector to the magnetopause using a minimum variance analysis of the magnetic field measurements [*Sonnerup and Cahill*, 1967]. Figure 14 shows the six normal vectors and the extrapolated magnetopause profile (in the satellite frame). A surface wave clearly affects the magnetopause. Its wavelength calculated using the plasma velocity measured by Geotail when it crosses the magnetopause
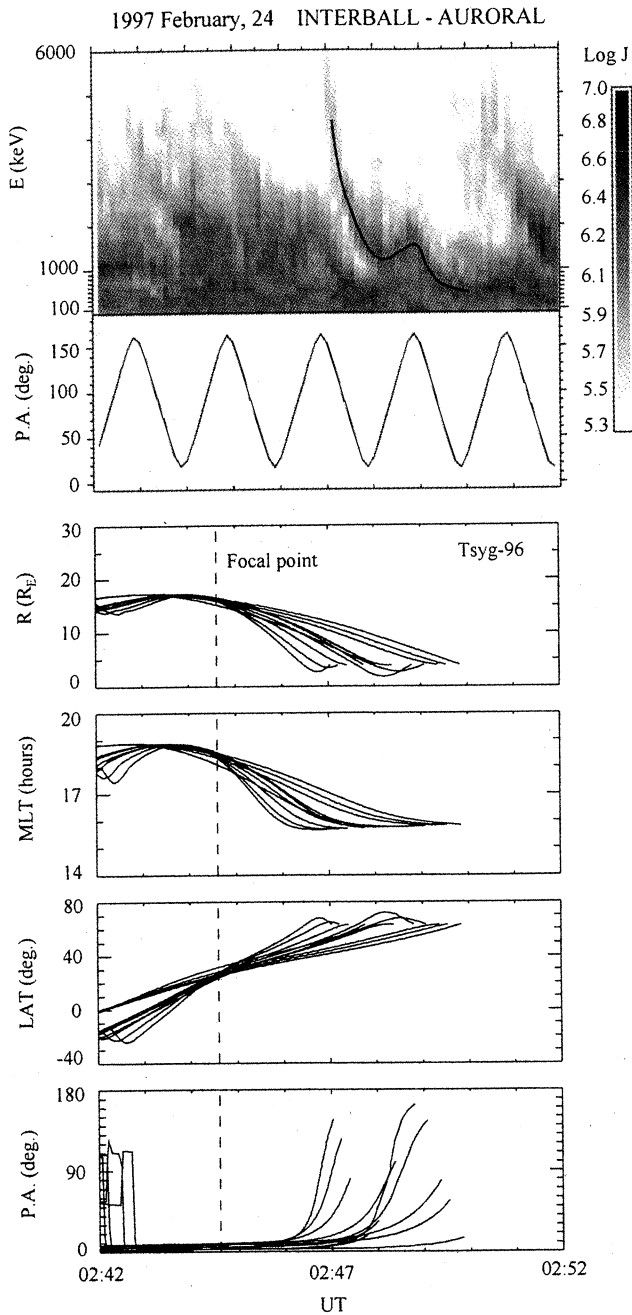
1997 February, 24   INTERBALL - AURORAL

24 FEBRUARY 1997

Figure 13. Same as Figure 10 for the injection event on February 24, 1997. The correlation coefficient reaches 0.7.

Figure 12. Backward computation for the injection beginning at 0227 on February 24, 1997 (noted B in Plate 2). Same presentation as Figure 9.

(~200 to 250 km s⁻¹) and the time delay between two boundary crossings (~6 to 7 min) reaches about 13 R_E. Both the shape and the wavelength of the wave are compatible with those expected from the Kelvin-Helmholtz instability. This result is similar to that of *Chen et al.* [1993] who found on the magnetopause dawn flank (X_{GSM}=-16 R_E, Y_{GSM}=-17 R_E), a wavelength of about 15 R_E. The shape of the magnetopause surface wave is similar to that given by MHD model [*Miura*, 1995].

As for the July 25, 1997, case, IA detected long-period waves (Figure 15). A wavelet analysis on the B field components in a magnetic field-aligned frame between 0230 and 0320 UT gives a period of around 250 s. The polarization is here linear and mainly oriented east-west but with the presence of a north-south component. *Potemra and Blomberg* [1996]
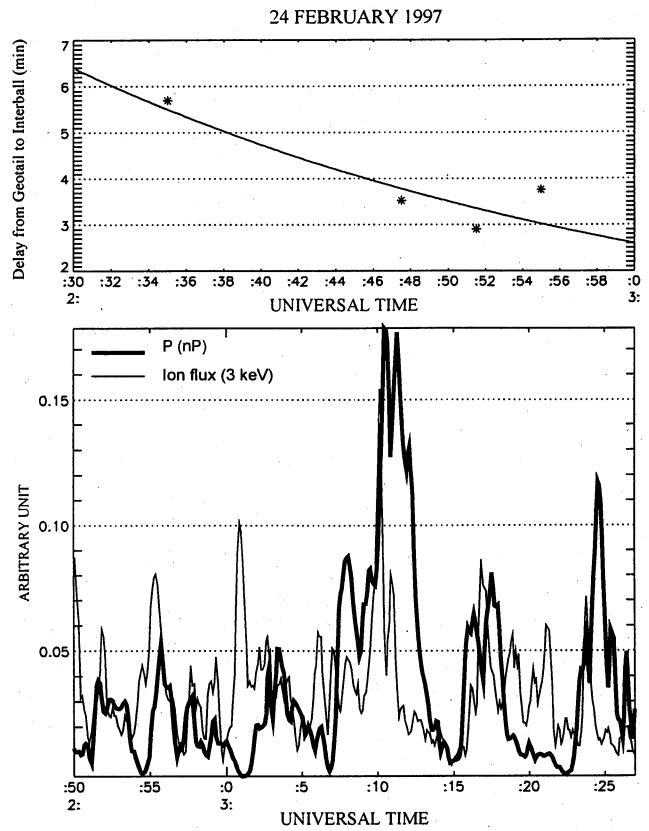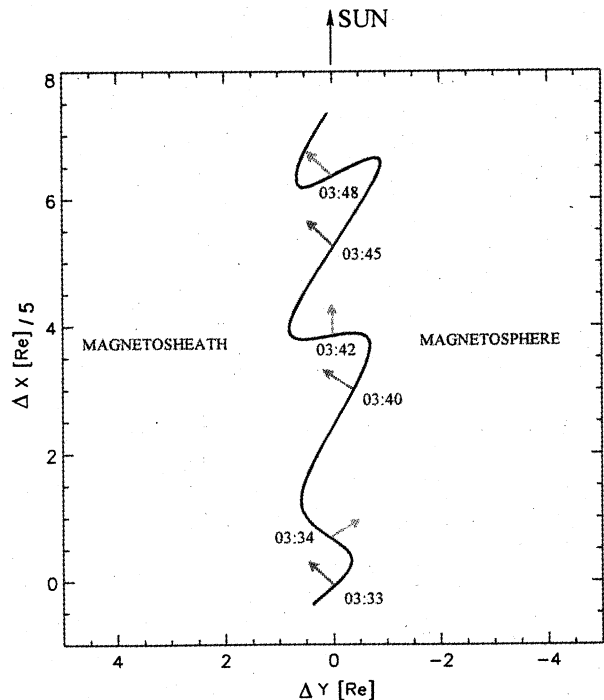

Figure 14. Normal of the magnetopause in the equatorial plane for the crossing pertaining to the period 0333 to 0348 on February 24, 1997. The extrapolated shape of the magnetopause is shown as a continuous line.
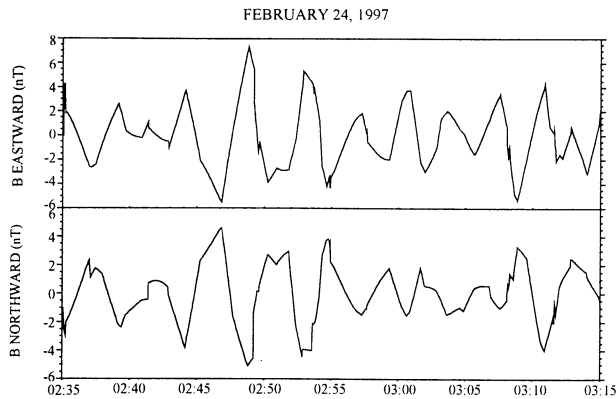
FEBRUARY 24, 1997

Figure 15. Residuals of the eastward and northward magnetic field measured on board Interball-Auroral between 0230 and 0320 UT on February 24, 1997.

have determined from the Viking electric and magnetic measurements that Pc5 pulsations often occur on geomagnetic field lines that guide Region 2 of field-aligned current. These waves have a linear polarization, oriented close to the geomagnetic east-west for the morningside and oriented east-west with the presence of a geomagnetic north-south component for eveningside, as is the case here. However, the study of *Potemra and Blomberg* [1996] focused on waves located 2°-10° equatorward of the boundary of Region 1 and Region 2 of currents, that is, in our Zone 2 or Zone 3. *Potemra et al.* [1989] showed from IMP8 observations in the solar wind that variations with a 4 min period in the solar wind density were directly responsible for the ULF waves observed by Active Magnetospheric Particle Tracer Explorers (AMPTE/CCE) and Viking spacecrafts and on the ground by the European Incoherent Scatter magnetometer array. *Nosé et al.* [1998] performed a study of the MLT dependence of the occurrence of Pc5 pulsations. They found that Pc5 pulsations are frequently observed between 0600 and 1900 MLT, with an occurrence peak in the late morning sector (0700-1000 MLT). This result is similar to the MLT dependence of ion injections observed by IA. In this interpretation framework, waves observed by IA are Pc5 pulsations related to instabilities resulting from magnetosheath pressure pulses.

6. Discussion and Conclusion

In the dawn and dusk auroral oval the Interball-Auroral satellite often crosses three zones with distinct plasma characteristics but clearly linked to each other. Indeed, the electron energy increases progressively from Zone 1 to Zone 3 and the ion injections observed in the first zone can continue in the two others. However, the injections observed in the equatorward part of Zone 2 and injections in Zone 3 quite often appear as bouncing ion clusters with no relation with nightside magnetic activity. Zone 1 is only detected at high latitudes (ILAT> 75°). Here the temperature of the ions is similar to that of the magnetosheath ions. The source of these events is the flank LLBL or the magnetosheath. A statistics on the components of the interplanetary magnetic field indicates that the injections mainly correspond to northward IMF. We also notice that Zone 1 is more frequently observed during periods where IMF tends to be radially directed (large $|B_x/B_y|$ ratio). Moreover, a clear correlation emerges between ion injections inside the high-latitude auroral region and the dynamic pressure variations in the magnetosheath. Such observations favor an

entry mechanism based on impulsive penetration. *Fairfield et al.* [1990] and *Sibeck* [1990] showed that pressure pulses observed in the magnetosheath are formed in the foreshock region. Because of the spiral nature of the IMF, the foreshock is more frequent for a quasi-parallel bow shock and then pressure pulses affect more the dawnside magnetopause. This could explain why injection events are more frequent in the auroral dawn magnetosphere.

Geotail data were used to demonstrate the presence of magnetopause surface waves likely due to Kelvin-Helmholtz instability, which could play a role in the occurrence of injections events observed by IA. The analysis of the magnetic field measured on board IA reveals characteristic waves associated with the ion injections. These waves are Pc5 pulsations with an azimuthal polarization for dawn events and mainly azimuthal with a radial component for dusk events. Our results extend the work by *Clemmons et al.* [1995] showing that particles can be injected in the morning auroral region from a quasi-periodic source located in the outer flank magnetosphere. The determination of the physical nature of the processes leading to the particle entry mechanism into the magnetosphere remains to be elucidated. The next research should also attack the problem to determine what is the potential importance of the injections reported in this paper to explain the plasma sheet population with magnetosheath plasma. This should be resolved using multispacecraft in situ measurements of the plasma entry mechanisms near the flank magnetopause.

References

Arshinkov, I. S., Z. N. Zhuzgov, A. Bochev, E. Zakharieva, V. Velev, V. A. Styazhkin, P. T. Baynov, and N. Abadgiev, Magnetic field experiment in the Interball project (experiment IMAP), *in Interball Mission and Payload*, edited by RKA, IKI and CNES, p. 222, Toulouse, France, 1995.

Carlson, C. W., and R. B. Torbert, Solar wind ion injections in the morning auroral oval, *J. Geophys. Res.*, *85*, 2903, 1980.

Chen, S.-H., M. G. Kivelson, J. T. Gosling, R. J. Walter, and A. J. Lazarus, Anomalous aspects of magnetosheath flow and of the shape and oscillations of the magnetopause during an interval of strongly northward interplanetary magnetic field, *J. Geophys. Res.*, *98*, 5727, 1993.

Clemmons, J. H., C. W. Carlson, and M. H. Boehm, Impulsive ion injections in the morning auroral region, *J. Geophys. Res.*, *100*, 12,133, 1995.

de la Beaujardiere, O., J. Watermann, P. Newell, and F. Rich, Relationship between Birkeland current regions, particle precipitation, and electric field, *J. Geophys. Res.*, *98*, 7711, 1993.

Delcourt, D. C., C. R. Chappell, T. E. Moore, and J. H. Waite Jr., A three-dimensional numerical model of ionospheric plasma in the magnetosphere, *J. Geophys. Res.*, *94*, 11,893, 1989.

Fairfield, D. H., W. Baumjohann, G. Paschmann, H. Lühr, and D. G. Sibeck, Upstream pressure variations associated with the bow shock and their effects on the magnetosphere, *J. Geophys. Res.*, *95*, 3773, 1990.

Farrugia, C. J., P. E. Sandholt, N. C. Maynard, W. J. Burke, J. D. Scudder, D. M. Ober, J. Moen, and C. T. Russel, Pulsation midmorning auroral arcs, filamentaion of a mixing region in a

boundary layer, and ULF waves observed during a Polar-Svalbard conjunction, *J. Geophys. Res., 105*, 27,531, 2000.

Frank, L. A., Plasma in the Earth's polar magnetosphere, *J. Geophys. Res., 76*, 5202, 1971.

Galperin, Y. I., N. V. Jorjio, R. A. Kovrazhkin, F. Cambou, J. A. Sauvaud, and J. Casnier, On the origin of auroral protons at the dayside auroral oval, *Ann. Geophys., 32*, 117, 1976.

Galperin, Y. I., V. A. Gladyshev, N. V. Jorjio, R. A. Kovrazhkin, N. V. Sinitsin, F. Cambou, J. A. Sauvaud, and J. Casnier, Adiabatic acceleration induced by convection in the plasmasheet, *J. Geophys. Res., 83*, 2567, 1978.

Klimov, S., et al., Aspi experiment: Measurements of fields and waves onboard the Interball-Tail mission, in *Interball Mission and Payload*, edited by RKA, IKI and CNES, p. 222, Toulouse, France, 1995.

Kokubun, S., T. Yamamoto, M. H. Acuña, K. Hayashi, K. Shiokawa, and H. Kawano, The Geotail magnetic field experiment, *J. Geomagn. Geoelectr., 46*, 7, 1994.

Kovrazhkin, R. A., J.-A. Sauvaud, and D. C. Delcourt, Interball-Auroral observations of 0.1-12 keV ion gaps in the diffuse auroral zone, *Ann. Geophysi., 17*, 734, 1999.

Lepping, R. P., et al., The Wind magnetic field investigation, *Space Sci. Rev., 71*, 207, 1995.

Lin, R. P., et al., A three-dimensional plasma and energetic particle investigation for the Wind spacecraft, *Space Sci. Rev., 71*, 125, 1995.

Lutsenko, V. N., J. Rojko, K. Kudela, T. V. Gretchko, J. Bala , J. Matišin, E. T. Sarris, K. Kalaitzides, and N. Paschalidis, Energetic particle experiment DOK-2 (Interball project), in *Interball Mission and Payload*, edited by RKA, IKI and CNES, p. 222, Toulouse, France, 1995.

Mitchell, D. G., F. Futchko, D. J. Williams, T. E. Eastman, L. A. Frank, and C. T. Russel, An extended study of the low-latitude boundary layer on the dawn and dusk flanks of the magnetosphere, *J. Geophys. Res., 92*, 7394, 1987.

Miura, A., Kelvin-Helmholtz instability at the magnetopause: Computer simulations, in *Physics of the Magnetopause, Geophys. Monogr. Ser.,* vol. 90, edited by P. Song et al., p. 285, AGU, Washington, D. C., 1995.

Mukai, T., S. Machida, Y. Saito, M. Hirahara, T. Terasawa, N. Kaya, T. Obara, M. Ejiri, and A. Nishida, The low-energy particle (LEP) experiment onboard the Geotail satellite, *J. Geomagn. Geoelectr., 46*, 669, 1994.

Newell, P. T., and C.-I. Meng, Mapping the dayside ionosphere to the magnetosphere according to particle precipitation characteristics, *Geophys. Res. Lett., 19*, 609, 1992.

Newell, P. T., W. J. Burke, E. R. Sanchez, C.-I. Meng, M. E. Greenspan, and C. R. Clauer, The low-latitude boundary layer and the boundary plasma sheet at low altitude: Prenoon precipitation regions and convection reversal boundaries, *J. Geophys. Res., 96*, 21013, 1991.

Nishikawa, K.-I., Particle entry through reconnection grooves in the magnetopause with a dawnward IMF as simulated by a 3-D EM particle code, *Geophys. Res. Lett., 25*, 1609, 1998.

Nosé, M., T. Iyemori, M. Sugiura, J. A. Slavin, R. A. Hoffman, J. D. Winningham, and N. Sato, Electron precipitation accompanying Pc5 pulsations observed by the DE satellites and at ground station, *J. Geophys. Res., 103*, 17,587, 1998.

Ober, D. M., N. C. Maynard, W. J. Bruke, J. Moen, A. Egeland, P. E. Sandholt, C. J. Farrugia, E. J. Weber, and I. D. Scudder, Mapping prenoon auroral structures to the magnetosphere, *J. Geophys. Res., 105*, 27,519, 2000.

Potemra, T. A., and L. G. Blomberg, A survey of Pc5 pulsations in the dayside high-latitude regions observed by Viking, *J. Geophys. Res., 101*, 24,801, 1996.

Potemra, T. A., H. Lühr, L. J. Zanetti, K. Takahashi, R. E. Erlandson, G. T. Marklund, L. P. Block, L. G. Blomberg, and R. P. Lepping, Multisatellite and ground-based observations of transient ULF waves, *J. Geophys. Res., 94*, 2543, 1989.

Russell, C. T., J. G. Luhmann, T. J. Odera, and W. F. Stuart, The rate of occurrence of dayside Pc3, 4 pulsations: The *L* value dependence of the IMF cone angle effect, *Geophys. Res. Lett., 10*, 663, 1983.

Sandahl, I., H. E. J. Koskinen, A. M. Mälkki, T. I. Pulkkinen, E. Y. Budnik, A. O. Fedorov, L. A. Frank, and J. B. Sigwarth, Dispersive magnetosheath-like ion injections in the evening sector on January 11, 1997, *Geophys. Res. Lett., 25*, 2568, 1998.

Sauvaud, J. A., J. Crasnier, K. Mouala, R. A. Kovrazkin, and N. V. Jorjio, Morning sector ion precipitation following substorm injections, *J. Geophys. Res., 86*, 3430, 1981.

Sauvaud, J. A., H. Barthe, C. Aoustin, J. J. Thocaven, J. Rouzaud, E. Penou, D. Popescu, R. A. Kovrazhkin, and K. G. Afanasiev, The ION experiment onboard the Interball-Auroral satellite; initial results on velocity-dispersed structures in the cleft and inside the auroral oval, *Ann. Geophys., 16*, 1056, 1998.

Sauvaud, J. A., D. Popescu, D. C. Delcourt, G. K. Parks, M. Brittnacher, V. Sergeev, R. Kovrazhkin, T. Mukai, and S. Kokubun, Sporadic plasma sheet ion injections into the high-altitude auroral bulge: Satellite observations, *J. Geophys. Res., 104*, 28,565, 1999.

Shue, J. H., J. K. Chao, H. C. Fu, C. T. Russel, P. Song, K. K. Khurana, and H. J. Singer, A new functional form to study the solar wind control of the magnetopause size and shape, *J. Geophys. Res., 102*, 9497, 1997.

Shue, J. H., et al., Magnetopause location under extreme solar wind conditions, *J. Geophys. Res., 103*, 17,691, 1998.

Sibeck, D. G., A model of the transient magnetospheric response to sudden solar wind dynamic pressure variations, *J. Geophys. Res., 95*, 3755, 1990.

Sibeck, D. G., W. Baumjohann, and R. E. Lopez, Solar wind dynamic pressure variations and transient magnetospheric signature, *Geophys. Res. Lett., 16*, 13, 1989a.

Sibeck, D. G., et al., The magnetospheric response to 8-minute-period strong-amplitude upstream pressure variations, *J. Geophys. Res., 94*, 2505, 1989b.

Sonnerup, B .U. Ö., and L. J. Cahill, Magnetopause structure and attitude from Explorer 12 observations, *J. Geophys. Res., 72*, 171, 1967.

Tsyganenko, N. A., A magnetospheric magnetic field model with a warped tail current sheet, *Planet. Space Sci., 37*, 5, 1989.

Tsyganenko, N. A., Modeling the Earth's magnetospheric magnetic field confined within a realistic magnetopause, *J. Geophys. Res., 100*, 5599, 1995.

Tsyganenko, N. A., and D. P. Stern, Modeling the global magnetic field of the large-scale Birkeland currents systems, *J. Geophys. Res., 101*, 27,187, 1996.

White, W. W., G. L. Siscoe, G. M. Erickson, Z. Kaymaz, N. C. Maynard, K. D. Siebert, B. U. Ö. Sonnerup, and D. R. Weimer, The magnetospheric sash and the cross-tail S, *Geophys. Res. Lett., 25*, 1605, 1998.

Woch, J., and R. Lundin, Temporal magnetosheath plasma injection observed with Viking: A case study, *Ann. Geophys., 9*, 133, 1991.

Woch, J., and R. Lundin, Signatures of transient boundary layer processes observed with Viking, *J. Geophys. Res., 97*, 1431, 1992.

Woch, J., R. Lundin, T. A. Potemra, and M. Shapshak, The projection of the magnetospheric boundary layers to mid-altitudes, in *Physical Signatures of the Magnetospheric Boundary Layer Processes, Series C: Mathematical and Physical Sciences,* vol. 425, p. 83, edited by J. A. Holtet and A. Egeland, Kluwer Academic Publishers, Netherlands, 1994.

Zastenker, G. N., M. N. Nozdrachev, J. Safrankova, Z. Nemecek, K. I. Paularena, A. J. Lazarus, R. P. Lepping, and T. Mukai, Fast solar wind plasma and magnetic field variations in the magnetosheath, *Czech. J. Phys., 49*, 579, 1999.

N. Y. Buzulukova and R. A. Kovrazhkin, Space Research Institute (IKI), 117997, 84/32 Profsoyuznaya Str, Moscow, Russia.

D. C. Delcourt, Centre d'étude des Environnements Terrestres et Planétaires, 4 Avenue de Neptune, Saint-Maur des Fossés, 94107, France.

M. Fujimoto, Department of Earth and Planetary Sciences, Tokyo Institute of Technology, Ookayama, Meguro 152, Tokyo, Japan.

S. Kokubun, STE Lab., Nagoya Univ., Honohara, Toyokawa, Aichi 442, Japan.

R. P. Lepping, NASA Goddard Space Flight Center, Greenbelt, MD 20771.USA.

R. P. Lin, Space Science Laboratory, University of California, Berkeley, Berkeley CA 94720, USA.

T. Mukai, Institute of Space and Astronautical Science, 3-1-1 Yoshinodai, Sagamihara, Kangawa 229, Japan.

J.-A. Sauvaud and H. Stenuit, Centre d'Etude Spatiale des Rayonnements, 9 Avenue du Colonel Roche, 31028 Toulouse Cedex 4, France. (Helene.Stenuit@cesr.fr, sauvaud@cesr.fr)